This article appeared in Applied Physics Letters **121**(19), 192105 (2022) and may be found at https://doi.org/10.1063/5.0106886.

Formation of oriented layered MoS_2 from amorphous thin film revealed by polarized X-ray absorption spectroscopy

M. Krbal,* J. Prikryl, and V. Prokop
Center of Materials and Nanotechnologies (CEMNAT), Faculty of Chemical Technology, University of Pardubice, nam. Cs legii, 565, 530 02 Pardubice, Czech Republic

I. Pis and F. Bondino
CNR-IOM, TASC Laboratory, 34149 Basovizza (TS), Italy

A.V. Kolobov
Department of Physical Electronics, Institute of Physics, Herzen State Pedagogical University of Russia, St. Petersburg 191186, Russia
(Dated: September 24, 2022)

MoS_2 is a prototypical two-dimensional (2D) van der Waals (vdW) solid, where covalently bonded S-Mo-S triplets are held together by weaker vdW forces. In this work, we have studied structural transformation from a three-dimensional amorphous phase of MoS_2 into a layered vdW crystal using S $L_{2,3}$ edge X-ray absorption near-edge structure (XANES) spectroscopy with in-plane and out-of-plane polarized X-ray beam. The crystallization process started from an isotropic amorphous phase is accompanied by establishment of vdW interaction between covalently bonded layers, resulting in the anisotropic nature of the crystalline phase. We have disclosed that the preferential growth of MoS_2 layers along the (200) Bragg reflection commences immediately from the amorphous phase with no intermediate crystal orientations. We have additionally identified a unique signature in the S $L_{2,3}$ edge spectrum that is associated with vdW bonds and can be possibly used to determine sulfur-based single-layered and multi-layered transition metal dichalcogenides.

The interest in transition metal dichalcogenides (TMDC) for semiconductor technology applications has grown significantly since the recent discovery of unique properties of graphene [1]. Covalently bonded triplet layers separated by weak van der Waals gaps allow individual triplets to slide with respect to each other, making TMDC a good solid lubricant [2, 3]. Similarly, triplet layers can be easily exfoliated to create two-dimensional (2D) TMDC crystals, which is accompanied by a change from indirect to direct optical gap [4]. Interestingly, the photo- and electro-catalytically active centers are located at the edges of the individual triplet layers [5, 6], and basal planes are employed for field-effect transistors and photoelectric devices [4, 7]. Horizontally or vertically aligned layers can be controlled by methods and conditions of their synthesis. For example, the formation of nanoparticles, standing flakes or flat monolayers by chemical routes, such as chemical vapour deposition or atomic (CVD) layer deposition (ALD), can be driven by appropriate growth temperature and pressure conditions [8, 9]. The same effect was also observed for the thermolysis of ammonium thiomolybdates at different temperatures [10]. However, it still remains unclear how to grow TMDC over a large area with a perfect surface coverage. Recently, the preparation of well-ordered planar TMDC crystals through solid-state crystallization of an amorphous phase has shown its potential to conduct a precise thin film thickness with high density surface coverage [11–13].

Crystallization of MoS_2 , a typical TMDC representative, from the initially amorphous state was recently investigated using transmission electron microscopy (TEM). Detailed analyses of magnetron sputtered a-MoS_2 on pre-heated Si substrates to 300 °C revealed co-existence of differently oriented MoS_2 crystals, which was explained as a local branching process during crystal growth. In the first stage, covalently bonded layers were grown parallel to the substrate at the substrate / MoS_2 interface with a maximum thickness up to 10 nm, while subsequent growth caused lamellar structures deeper in the film perpendicular to the substrate [14, 15]. Additional annealing of a-MoS_2 at 500 °C under vacuum formed crystals randomly oriented through out the film thickness, even at the interface [14]. The recent report on crystallization of amorphous MoS_3 studied by TEM disclosed that grown MoS_2 crystals were oriented perpendicular to the substrate in the range of temperatures from 400 to 780 °C and the preferential crystal growth along the (002) crystallographic plane was exclusively formed above 780 °C [10].

Here we demonstrate the use of S $L_{2,3}$ edge X-ray absorption near-edge structure (XANES) spectroscopy with linearly polarized X-ray radiation to investigate the process of the formation of the ordered crystalline phase by means of solid-state crystallization of the amorphous phase. Thanks to the three-dimensional sensitivity of XANES independent of the presence of long-range order with the limited coherence length of $\approx$ 1 nm, this powerful technique can distinguish structural changes on an atomic scale even below the X-ray diffraction limit.

Experimental and simulation details can be found in the supplementary information.

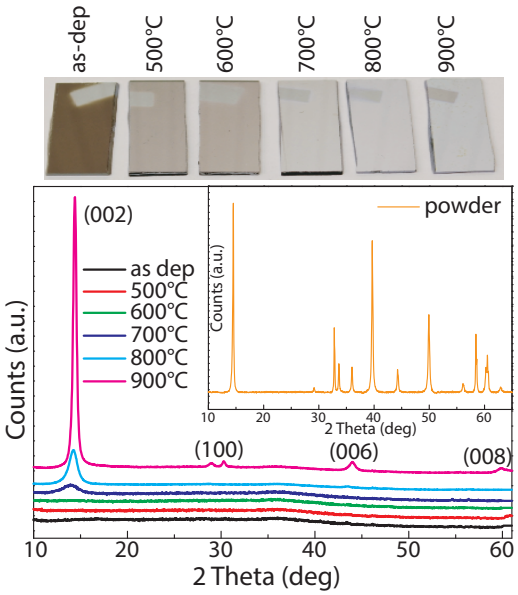

FIG. 1: (Color online) XRD patterns of the as-deposited and crystallized MoS_2 in the range of temperatures from 500 to 900 °C with a step of 100 °C. The inset figure represents the XRD pattern of the MoS_2 powder as a reference. The photographs above the graph show the color change of the annealed samples in the studied range of temperatures (MoS_2 thin films deposited on a Si wafer).

The amorphous nature of the as-deposited MoS_2 thin films was confirmed by XRD, as shown in Fig. 1. XRD analyses of ex-situ annealed MoS_2 thin films revealed that the first broad single reflection peak at about 2θ =13.9 deg emerges from the amorphous background for the sample annealed at 700 °C. The reflection peak corresponds well to the most intense reflection peak along the crystallographic plane (002), indicating that the amorphous MoS_2 begins to crystallize in the 2H-MoS_2 layered phase [16]. With increasing temperature from 700 °C, the Bragg reflection peak along the (002) crystallographic plane increases the intensity and the XRD pattern of the MoS_2 sample annealed at 900 °C is sufficiently developed to identify additional Bragg reflection lines at (006) and (008), characterizing the arrangement of the covalently bonded two-dimensional layers into a well-crystallized multilayer of MoS_2 with a strong preferential crystal growth of the 2H MoS_2 phase with the out-of-plane c-axis orientation (covalently bonded MoS_2 layers are parallel to the substrate) [13]. This observation is in good agreement with a recent study showing that Mo thin film sulfurization at 800 °C using a low heating rate induces exclusive growth of horizontally oriented MoS_2 crystals [17] but in sharp contrast with the XRD pattern of the reference MoS_2 powder, shown in the inset of Fig. 2, where randomly oriented MoS_2 crystals revealed further Bragg reflections [16].

While no Bragg reflection peaks on XRD patterns can be observed for samples annealed below 700 °C, the color change of MoS_2 samples annealed at different temperatures, shown above the fig. 1, is associated with a change in bonding nature [18]. The as-deposited amorphous MoS_2 (brown) contains a large number of homopolar Mo-Mo bonds, the intermediate phase (light brown) is mostly formed by heteropolar Mo-S bonds, and the final state (metallic-like) is represented by the 2H MoS_2 crystalline phase grown with basal planes parallel to the substrate surface.

Compared to XRD, XANES spectroscopy provides complex structural information that can be considered as a fingerprint of each structural arrangement. The ability to form vdW bonds in layered chalcogenides is due to the presence of pairs of non-bonding p-electrons (so-called lone-pair electrons), which can be therefore used to investigate the preferential crystal growth of MoS_2 via the S $L_{2,3}$ edge XANES spectroscopy with in-plane and out-of-plane polarized X-ray beam. The X-ray absorption spectra involve an electronic transition from a filled core level to an empty (conduction band) state. Due to the X-ray absorption selection rules, the S $L_{2,3}$ edge is represented by the symmetry allowed p-d absorption, corresponding to an electron transition from S 2p to S $4d - Mo$ 5p hybridized states at energies above $\approx$ 165 eV, while the characteristic pre-edge area (162-166 eV) is associated with probing S $3p - Mo$ 4d hybridized states. More details about the local projected density of states of crystalline MoS_2 can be found in [5].

Figure 2 demonstrates the variation of the S $L_{2,3}$ edge XANES spectra obtained with in-plane and out-of-plane polarized X-ray beam for the amorphous and annealed phases at temperatures of 500 and 900 °C including the S $L_{2,3}$ edge XANES spectra of randomly oriented crystalline MoS_2 flakes for comparison. Note, that the overall evolution of the S $L_{2,3}$ edge XANES spectra in the range of temperatures from 500 to 900 °C can be found in the supplementary information, fig. S2. One can see that the S $L_{2,3}$ edge XANES spectrum of the amorphous MoS_2 phase is a featureless and smooth curve in the entire studied energy range. On the other hand, weak characteristic peaks and oscillations can be observed on the S $L_{2,3}$ edge XANES spectrum for MoS_2 annealed at 500 °C. With further increasing annealing temperature, the intensity of individual peaks becomes more pronounced, indicating a gradual transformation into the layered 2H MoS_2 phase.

Of special interest is the revealing whether magnetron sputtered amorphous MoS_2 annealed at 500 °C under vacuum leads to isotropic crystallization [14], which is in our case below the detection limit of XRD and/ or if there is dominant in-plane crystal growth of MoS_2 layers started from 400 °C, which subsequently transforms to the out-of-plane orientation above 780 °C [10].

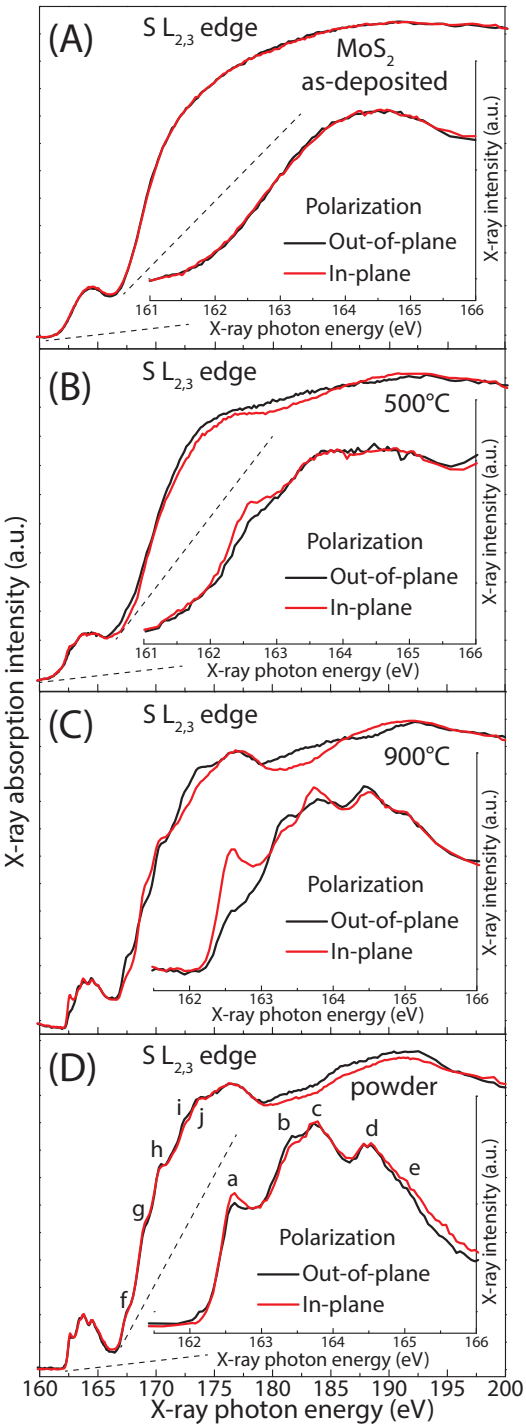

FIG. 2: The comparison of S $L_{2,3}$ edge XANES spectra from (A) the as deposited, (B) annealed at 500 °C, (C) annealed at 900 °C and (D) a randomly oriented MoS_2 powder obtained with incident photons polarized out-of-plane (black) and in-plane (red. Inset figures represent zoomed S $L_{2,3}$ edge XANES spectra of MoS_2 thin films.

For this purpose, a detailed analysis of polarization-dependent S $L_{2,3}$ edge XANES spectra was performed on as-deposited MoS_2 and annealed samples at 500 and 900 °C and compared to the randomly oriented crystalline MoS_2 flakes. As expected, isotropic structures such as as-deposited amorphous MoS_2 and randomly oriented crystalline MoS_2 flakes are insensitive to the polarized X-ray beam, which is demonstrated by the overlap of corresponding S $L_{2,3}$ edge XANES spectra obtained at both polarizations. On the other hand, MoS_2 thin films annealed at 500 and 900 °C clearly show systematic differences in the intensity of corresponding absorption peaks in the pre-edge area (a to e) and the absorption edge (f to j) and also oscillations above the absorption edge vary distinctly. In both cases, the trend in observed changes is the same, which in combination with XRD results allow us to draw a conclusion that the covalently bonded layers or their fragments (nuclei) are locally preferentially oriented parallel to the substrate even in the intermediate phase prepared by annealing at 500 °C. If crystalline fragments with basal planes oriented perpendicular to the substrate prevailed, the polarization vector of the incident photon beam would be parallel to the MoS_2 basal plane for both used polarizations and no linear dichroism would be observed. Based on the XANES and XRD we cannot exclude the possibility that some nanocrystals with different orientations may exist to a lesser extent. On the other hand, the formation of a horizontally oriented phase without intermediate crystal orientations is in accord with the crystallization of oriented MoS_2 prepared by sulfurization of predeposited Mo films [19].

We now turn to the most intriguing finding of this work. Focusing on the pre-edge area, the intensity of the first peak was found to be strongly sensitive to polarization of the incident X-ray beam (see fig.2 (C)). The origin of this absorption was described as the electron transition from S $2p_{3/2}$ to S $3p - Mo$ 4d hybridized states [5]. Using the FEFF code applied to a single- and two- layered 2H MoS_2 phase, shown in Fig. 3, we found that the pre-edge of the S $L_{2,3}$ edge XANES spectra calculated at both polarizations for the 1L MoS_2 do not change significantly and the characteristic intense peak has low intensity. Surprisingly, a similar effect was obtained for the S atom located at the top of the first layer of 2L MoS_2 , which is however accompanied by larger differences between in-plane and out-of-plane polarizations. On the other hand, the intense first peak is more developed on the S $L_{2,3}$ edge XANES spectra calculated for the S atom pointing to the vdW gap in 2L MoS_2 and at the same time the intensity change under the polarized X-ray radiation is in accordance with the experimentally obtained S $L_{2,3}$ edge XANES spectra of crystalline MoS_2 . Conclusions from the recently simulated S $L_{2,3}$ edge XANES spectra also confirm the presence of this peak in the pre-edge area for a bulk MoS_2 phase, while it is missing on

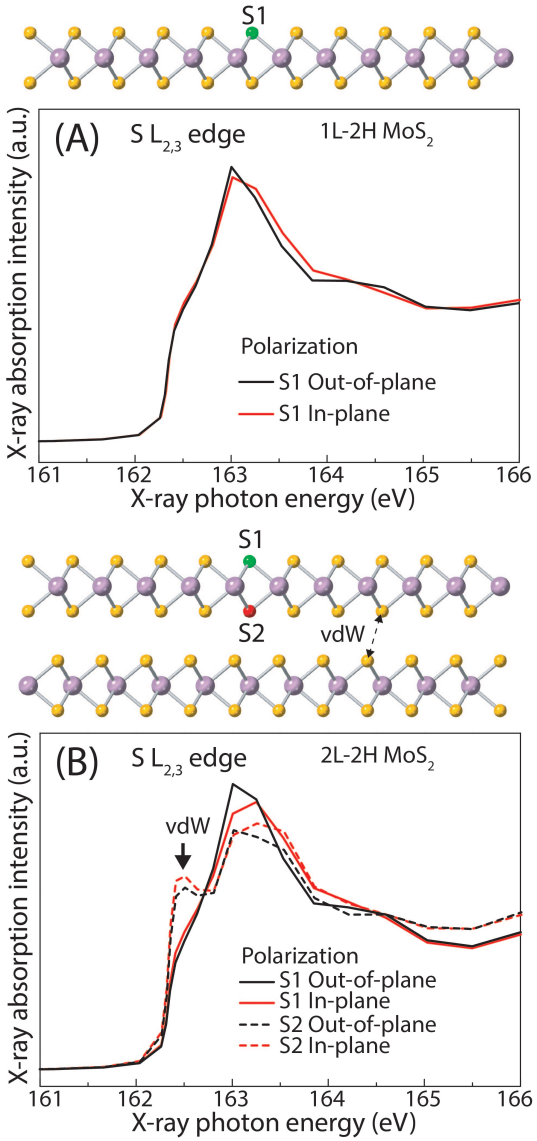

FIG. 3: FEFF simulations of S $L_{2,3}$ edge XANES spectra of (A) mono-layer and (B) two-layer MoS_2 using X-ray radiation polarized in-plane (red) and out of the MoS_2 basal plane (black).

S $L_{2,3}$ edge XANES spectrum for the a mono-layer of MoS_2 [20], which is nevertheless in contrast with other report, claiming no significant difference in the spectral shape of S $L_{2,3}$ edge for the mono-layer and the bulk of MoS_2 [5].

Interestingly, recently reported experimental data demonstrated the non-negligible contribution of vdW interaction to the increase in the intensity of the first peak in the pre-edge area on the S $L_{2,3}$ edge XANES spectrum for the S atom at the MoS_2/SiO_2 interface [21]. We therefore hypothesize that the increased intensity of the the first peak can be a signature of the vdW gap in the 2H layered MoS_2 phase and hence one may possibly differentiate mono- and more- layered MoS_2 structures. This hypothesis should be verified in the future by a non-trivial experiment dealing with a suspended mono-layer and few-layer MoS_2 crystal [22].

There is another important conclusion. Since the first intense peak on the pre-edge S $L_{2,3}$ edge XANES spectrum is evident even for MoS_2 thin films annealed at 500 °C, it seems that crystallization nuclei in the amorphous phase always incubate as few-layered structures rather than large mono-layered sheets, which are subsequently organized in the layered phase at elevated temperatures.

In conclusion, we have performed polarization-dependent S $L_{2,3}$ edge XANES spectroscopy to study the formation of vdW MoS_2 anisotropic crystals through solid-state crystallization from a three-dimensional isotropic amorphous phase. Our results demonstrate strong preferential crystal growth of MoS_2 layers along the (200) Bragg reflection, which begins immediately from the amorphous phase. Using FEFF simulations, we have further disclosed a characteristic fingerprint in the pre-edge area of S $L_{2,3}$ XANES spectrum of MoS_2 that can be associated with the presence of vdW bonding. We believe that our findings can also help to distinguish between mono-and multi-layered transition metal dichalcogenides.

See the supplementary material for the information regarding the experimental and simulation details and the temperature evolution of polarized S $L_{2,3}$ edge XANES spectra of MoS_2 thin films.

This work was supported by the Czech Science Foundation 19-17997S, the Ministry of Education, Youth and Sports (LM2018103). I.P. acknowledges funding from EUROFEL project and Elettra Sincrotrone Trieste for providing access to synchrotron radiation facilities. AVK is grateful to the Russian Science Foundation for partial support of this work under grant 22-19-00766.

The data that support the findings of this study are available from the corresponding author upon reasonable request.

* Milos.Krbal@upce.cz

[1] S. Pisana, M. Lazzeri, C. Casiraghi, K. S. Novoselov, A. K. Geim, A. C. Ferrari, and F. Mauri, Nature Materials **6**, 198 (2007), ISSN 1476-4660, URL https://doi.org/10.1038/nmat1846.

[2] L. Rapoport, Y. Bilik, Y. Feldman, M. Homyonfer, S. R. Cohen, and R. Tenne, Nature **387**, 791 (1997), ISSN 1476-4687, URL https://doi.org/10.1038/42910.

[3] P. Serles, E. Nicholson, J. Tam, N. Barri, J.-B. Chemin, G. Wang, Y. Michel, C. V. Singh, P. Choquet, A. Saulot, et al., Advanced Functional Materials **n/a**, 2110429 (2022), https://onlinelibrary.wiley.com/doi/pdf/10.1002/adfm.202110429, URL https://onlinelibrary.wiley.com/doi/abs/10.1002/adfm.202110429.

[4] A. V. Kolobov and J. Tominaga, *Two-dimensional Transition-Metal Dichalcogenides* (Springer Series in Materials Science, Springer International Publishing AG, 2016).

[5] A. Parija, Y.-H. Choi, Z. Liu, J. L. Andrews, L. R. De Jesus, S. C. Fakra, M. Al-Hashimi, J. D. Batteas, D. Prendergast, and S. Banerjee, ACS Cent. Sci. **4**, 493 (2018), ISSN 2374-7943, URL https://doi.org/10.1021/acscentsci.8b00042.

[6] F. Jaramillo Thomas, P. Jorgensen Kristina, B. Jacob, H. Nielsen Jane, H. Sebastian, and C. Ib, Science **317**, 100 (2022), URL https://doi.org/10.1126/science.1141483.

[7] A. Sebastian, R. Pendurthi, T. H. Choudhury, J. M. Redwing, and S. Das, Nature Communications **12**, 693 (2021), ISSN 2041-1723, URL https://doi.org/10.1038/s41467-020-20732-w.

[8] M. He, F. Kong, G. Yin, Z. Lv, X. Sun, H. Shi, and B. Gao, RSC Adv. **8**, 14369 (2018), URL http://dx.doi.org/10.1039/C8RA01147H.

[9] L. Liu, R. Gao, Y. Xing, and Z. Wu, ACS Appl. Nano Mater. **5**, 5652 (2022), URL https://doi.org/10.1021/acsanm.2c00439.

[10] L. Fei, S. Lei, W.-B. Zhang, W. Lu, Z. Lin, C. H. Lam, Y. Chai, and Y. Wang, Nature Communications **7**, 12206 (2016), ISSN 2041-1723, URL https://doi.org/10.1038/ncomms12206.

[11] J.-H. Huang, H.-H. Hsu, D. Wang, W.-T. Lin, C.-C. Cheng, Y.-J. Lee, and T.-H. Hou, Sci Rep **9**, 8810 (2019).

[12] M. Krbal, V. Prokop, A. A. Kononov, J. R. Pereira, J. Mistrik, A. V. Kolobov, P. J. Fons, Y. Saito, S. Hatayama, Y. Shuang, et al., ACS Appl. Nano Mater. **4**, 8834 (2021), URL https://doi.org/10.1021/acsanm.1c01504.

[13] M. Krbal, V. Prokop, J. Prikryl, J. R. Pereira, I. Pis, A. V. Kolobov, P. J. Fons, Y. Saito, S. Hatayama, and Y. Sutou, Crystal Growth & Design (2022), ISSN 1528-7483, URL https://doi.org/10.1021/acs.cgd.1c01504.

[14] J. Moser and F. Levy, Journal of Materials Research **7**, 734 (1992), ISSN 0884-2914, URL https://www.cambridge.org/core/article/growth-mechanisms-and-nearinterface-structure-in-relati BDE97DA487E2CFE4AA6DA9E9D7F13C78.

[15] T. Ohashi, K. Suda, S. Ishihara, N. Sawamoto, S. Yamaguchi, K. Matsuura, K. Kakushima, N. Sugii, A. Nishiyama, Y. Kataoka, et al., Japanese Journal of Applied Physics **54**, 04DN08 (2015), ISSN 1347-4065, URL http://dx.doi.org/10.7567/JJAP.54.04DN08.

[16] M. S. Whittingham and F. R. Gamble Jr., Mat. Res. Bull. **10**, 363 (1975).

[17] M. Sojkova, K. Vegso, N. Mrkyvkova, J. Hagara, P. Hutar, A. Rosova, M. Caplovicov, U. Ludacka, V. Skakalova, E. Majkova, et al., RSC Adv. **9**, 29645 (2019), URL http://dx.doi.org/10.1039/C9RA06770A.

[18] M. Krbal, J. Prikryl, I. Pis, V. Prokop, J. Rodriguez-Pereire, A. Kolobov, and P. Fons, Journal of Alloys and Compounds (2022).

[19] A. Shaji, K. Vegso, M. Sojkova, M. Hulman, P. Nadazdy, P. Hutar, L. Pribusova Slusna, J. Hrda, M. Bodik, M. Hodas, et al., J. Phys. Chem. C **125**, 9461 (2021), ISSN 1932-7447, URL https://doi.org/10.1021/acs.jpcc.1c01716.

[20] M. Dadsetani, H. Nejatipour, and T. Nouri, Physica E: Low-dimensional Systems and Nanostructures **73**, 198 (2015), ISSN 1386-9477, URL https://www.sciencedirect.com/science/article/pii/S1386947715300606.

[21] M. Lee, Y. Kim, A. Y. Mohamed, H.-K. Lee, K. Ihm, D. H. Kim, T. J. Park, and D.-Y. Cho, ACS Appl. Mater. Interfaces **12**, 53852 (2020), ISSN 1944-8244, URL https://doi.org/10.1021/acsami.0c17544.

[22] H. Shi, R. Yan, S. Bertolazzi, J. Brivio, B. Gao, A. Kis, D. Jena, H. G. Xing, and L. Huang, ACS Nano **7**, 1072 (2013), ISSN 1936-0851, URL https://doi.org/10.1021/nn303973r.